Available online at www.sciencedirect.com
ScienceDirect
Biochemical and Biophysical Research Communications 351 (2006) 1–6
BBRC
www.elsevier.com/locate/ybbrc

Structure of the POZ domain of human LRF, a master regulator of oncogenesis

Florian D. Schubot, Joseph E. Tropea, David S. Waugh *

Macromolecular Crystallography Laboratory, National Cancer Institute at Frederick, P.O. Box B, Frederick, MD 21702-1201, USA

Received 18 September 2006
Available online 9 October 2006

Abstract

The proto-oncogenic properties of the POK family of transcriptional repressors BCL6, PLZF, and LRF have been well established. These proteins utilize their amino-terminal POZ domains for multimerization and the recruitment of co-repressors. Because LRF represses the production of the tumor suppressor $p19^{Arf}$ (ARF), it is regarded as an attractive therapeutic target for the treatment of many types of cancer. The crystal structure of the LRF POZ domain reveals a high degree of structural conservation with the corresponding domains of BCL6 and PLZF. However, striking differences between the electrostatic properties of the BCL6 and LRF POZ domains suggest that if, like BCL6, LRF interacts with the co-repressor SMRT, it almost certainly uses a different mechanism to do so. These differences may also explain why LRF interacts with BCL6 but not with PLZF. Finally, the conservation of crystal packing contacts suggests the probable location of the interface that mediates LRF/BCL6 complex formation.
Published by Elsevier Inc.

Keywords: POK; POZ; BTB; Krüppel; LRF; FBI-1; Pokemon; PLZF; BCL6; SMRT

POK (POZ and Krüppel) family proteins are ubiquitous transcriptional repressors. Several of them have been shown to play central roles in human cell differentiation and development [1–3]. Furthermore, oncogenic properties have been attributed to POK proteins BCL6 (B-cell lymphoma 6) [4–6], PLZF (promyelocytic leukemia zinc finger) [7], and, most recently, LRF (leukemia/lymphoma related factor; also known as OCZF, FBI-1, and pokemon) [8,9]. POK proteins have a modular architecture consisting of two domains separated by a long, possibly unstructured linker. The carboxy-terminal Krüppel-type zinc finger domains bind to DNA at specific consensus sequences upstream of transcription initiation sites. The amino-terminal domains of POK family proteins are known as POZ (poxvirus and zinc finger) or BTB (bric-a-brac tramtrack broad complex) domains [10]. The POZ domain mediates homodimerization and oligomerization [10]. The POZ domain also facilitates the recruitment of co-repressor proteins such as SMRT [11], N-CoR [12], BcoR [13], and mSin3A [12,14] as well as class I and II histone deacetylases [12,14,15].

LRF directly represses transcription of the tumor suppressor gene *ARF*, thereby promoting tumor growth [9]. The oncogenic properties of the related POK protein BCL6 are greatly enhanced by LRF [9]. BCL6 and LRF have been shown to interact with themselves as well as each other by yeast two-hybrid studies [1]. However, while homodimerization depended only on their POZ domains, the formation of heterodimers required the full-length proteins [1]. Curiously, the same study failed to detect an interaction between LRF and PLZF, another POK protein that is even more closely related to LRF than is BCL6 (Fig. 1A). The crystal structures of the POZ domains of BCL6 (POZ^{BCL6}) [16] and PLZF (POZ^{PLZF}) [17,18] have been reported previously. The structure of the POZ^{BCL6} domain in complex with a peptide constituting the SMRT-binding epitope has also been published [16].

* Corresponding author. Fax: +1 301 846 7148.
E-mail address: waughd@ncifcrf.gov (D.S. Waugh).

0006-291X/$ - see front matter Published by Elsevier Inc.
doi:10.1016/j.bbrc.2006.09.167

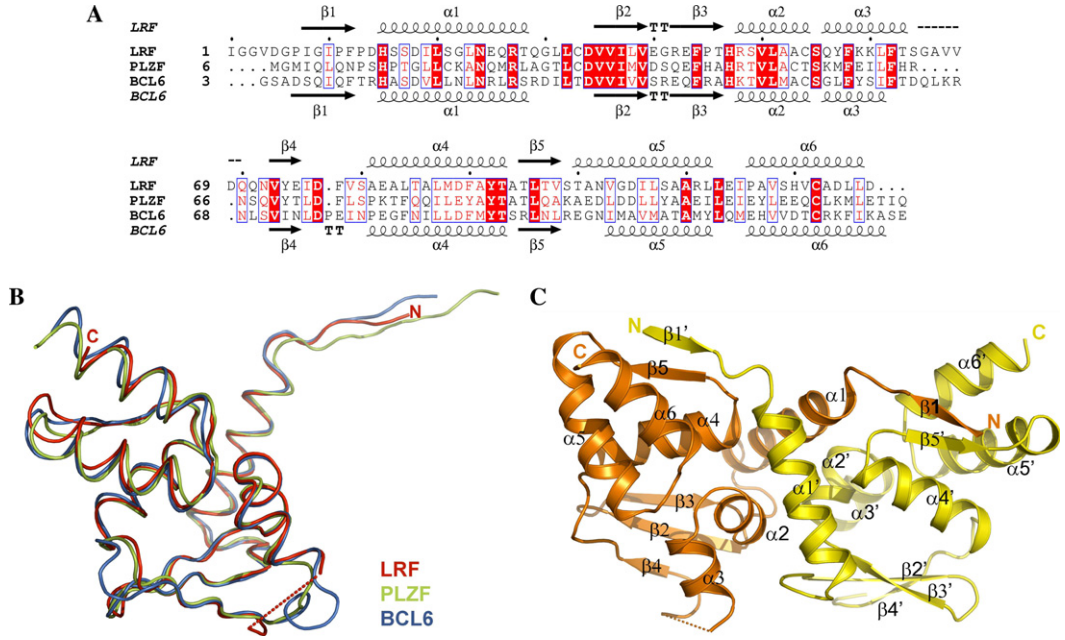

Fig. 1. The POZ^{LRF} structure. (A) ESPRIPT-generated [32] structure-based sequence alignment of POZ^{LRF}, POZ^{BCL6}, and POZ^{PZLF}. The secondary structures of POZ^{LRF} and POZ^{BCL6} are displayed above and below the alignment, respectively. (B) Backbone superposition of the POZ domains of LRF, BCL6, and PLZF. (C) Ribbon model of the dimeric POZ^{LRF} domain.

Here, we report the crystal structure of the POZ domain of the human proto-oncogene LRF (POZ^{LRF}). We compare and contrast its structure with those of the POZ^{BCL6} and POZ^{PLZF} domains, and speculate about the structural basis for similarities and differences between their roles in hetero-oligomerization and the recruitment of co-repressors.

Materials and methods

Cloning, expression, and purification. The POZ domain of human LRF was amplified from Image clone ID 6379572 (American Type Culture Collection, Manassas, VA) by the polymerase chain reaction (PCR) using the following oligonucleotide primers: 5′-GAGAACCTGTACTTCCAGGCCGGCGGCGTGGACGGCCCCATC-3′ and 5′-GGGGACCACTTTGTACAAGAAAGCTGGGTTATTAGTCCAGGAGGTCGGCGCACACGTG-3′ (primer R). The PCR amplicon was subsequently used as template for a second PCR with the following primers: 5′-GGGGACAAGTTTGTACAAAAAAGCAGGCTCGGAGAACCTGTACTTCCAG-3′ and primer R. The amplicon from the second PCR was inserted by recombinational cloning into the entry vector pDONR201 (Invitrogen, Carlsbad, CA), and the nucleotide sequence confirmed. The open reading frame encoding POZ^{LRF} (A_2–D_{128}) and containing a recognition site (ENLYFQ/A) for tobacco etch virus (TEV) protease on its N-terminus was moved by recombinational cloning into the destination vector pDEST-HisMBP to produce pJT18. pJT18 directs the expression of POZ^{LRF} as a fusion to *Escherichia coli* maltose-binding protein (MBP) with an intervening TEV protease recognition site. The MBP contains an N-terminal hexahistidine tag for affinity purification by IMAC. The fusion protein was expressed in the *E. coli* strain BL21(DE3) (Novagen, Madison, WI). Cells containing the expression vector were grown to mid-log phase ($OD_{600} \sim 0.5$) at 37 °C in Luria broth containing 100 μg ml^{-1} ampicillin and 0.2% glucose. Overproduction of fusion protein was induced with isopropyl-β-D-thiogalactopyranoside at a final concentration of 1 mM for 4 h at 30 °C. The cells were pelleted by centrifugation and store at −80 °C.

All procedures were performed at 4–8 °C. Ten grams of *E. coli* cell paste was suspended in 50 mM sodium phosphate (pH 7.5), 200 mM NaCl, and 25 mM imidazole buffer (buffer A) containing 1 mM benzamidine HCl (Sigma Chemical Company, St. Louis, MO) and Complete EDTA-free protease inhibitor cocktail tablets (Roche Molecular Biochemicals, Indianapolis, IN). The cells were lysed with an APV-1000 homogenizer (Invensys, Roholmsvej, Germany) at 10,000 psi and centrifuged at 30,000*g* for 30 min. The supernatant was filtered through a 0.22 μm polyethersulfone membrane and applied to a 12 ml Ni–NTA superflow column (Qiagen, Valencia, CA) equilibrated in buffer A. The column was washed to baseline with buffer A and then eluted with a linear gradient of imidazole to 250 mM. Fractions containing recombinant His_6-MBP-POZ^{LRF} were pooled, concentrated using an Amicon YM10 membrane (Millipore Corporation, Bedford, MA), diluted with 50 mM sodium phosphate (pH 7.5), 200 mM NaCl buffer to reduce the imidazole concentration to about 25 mM, and digested overnight with His_6-tagged TEV protease. The digest was applied to a 50 ml Ni–NTA superflow column equilibrated in buffer A and the POZ^{LRF} domain emerged in the column effluent. The column effluent was incubated overnight with 10 mM dithiothreitol (DTT), concentrated as above, and applied to a HiPrep 26/60 Sephacryl S-100 HR column equilibrated in 25 mM Tris–HCl (pH 7.5), 150 mM NaCl, and 2 mM DTT. The peak fractions containing POZ^{LRF} were pooled and concentrated to 24–25 mg ml^{-1} (estimated at 280 nm using a molar extinction coefficient of 3840 M^{-1} cm^{-1}). Aliquots were flash-frozen in liquid nitrogen and stored at −80 °C. The final product was judged to be >95% pure by sodium dodecyl sulfate–polyacrylamide gel electrophoresis. The molecular weight of POZ^{LRF} was confirmed by electrospray mass spectroscopy.

Crystallization and X-ray data collection. Crystallization screening of the POZ^{LRF} sample was conducted in CrystalQuick round-bottomed plates (Hampton Research, Aliso Viejo, CA) using the sitting drop technique. Three different protein to precipitant ratios (4:1, 1:1, and 1:4) were screened with a Hydra II Plus One (Matrix Technologies) liquid handling robot. The sample was initially screened with commercially available crystallization matrices and crystals were obtained from condition 28 of the PEG/Ion crystallization Screen (Hampton Research, Aliso Viejo, CA). The initial crystal diffracted to weaker than 4 Å and therefore we screened for a suitable additive. Ultimately, optimized conditions that yielded the

Table 1
Data collection and refinement statistics

LRF	
(A) Data collection statistics	
Resolution (Å)	50–2.03
Wavelength (Å)	1.00
Space group	$I4_122$ (tetragonal)
Cell (Å)	$a = b = 65.8$; $c = 162.6$
Completeness (%) (last shell)[a]	98.2 (2.13–2.03:99.8)
Redundancy	13.4 (12.7)
I/σ_I	25.9 (8.8)
R_{merge} (%)[b]	9.6 (25.9)
(B) Refinement statistics	
Resolution range (Å)	50–2
R (%)[c]	22.9
R_{free} (%)[d]	29.1
rms bonds (Å)	0.017
rms angles (°)	1.60
Number of water molecules	123
Temperature factor (Å^2)	21.6
Number of protein atoms	1562
Number of solvent molecules	117
Ramachandran analysis (%)	
Most favored	91.2
Allowed	8.8
Disallowed	0

[a] Values in parentheses relate to the highest resolution shell.

[b] $R_{merge} = \sum|I| - \langle I\rangle/\sum I$, where I is the observed intensity, and $\langle I\rangle$ is the average intensity obtained from multiple observations of symmetry-related reflections after rejections.

[c] $R = \sum||F_o| - |F_c||/\sum|F_o|$, where F_o and F_c are the observed and calculated structure factors, respectively.

[d] R_{free} defined in Brunger [31].

tetragonal crystals used for the structure solution consisted of a 1:1 ratio of protein solution with a precipitant mixture containing 0.18 M calcium acetate, 18% PEG 3350, and 0.01 M praseodymium(III) acetate.

Crystals of POZ^{LRF} were mounted in a loop after soaking the crystal in a cryo-solution consisting of 90% crystallization stock solution and 10% glycerol, and subsequently flash-frozen in liquid nitrogen. The data set that was used to solve the structure was collected at the SER-CAT insertion device beamline (22-ID, Advanced Photon Source, Argonne National Laboratory) equipped with a MAR CCD 225 detector. Data processing was carried out with the HKL2000 program suite [19]. The details of data collection and processing are provided in Table 1.

Structure solution and refinement. The structure was solved by molecular replacement with the program PHASER [20] using the structure of POZ^{BCL6} as a search model. The structure was manually completed with the molecular modeling program O [21]. The model was refined with REFMAC [22] followed by manual adjustment against SIGMAA [23] weighted difference Fourier maps. After several rounds of manual adjustment and refinement, 117 water molecules were added to the structure using ARP/wARP [24] in combination with REFMAC.

Model quality was assessed with PROCHECK [25]. All non-glycine residues in the structure resided either in the most favorable or in the allowed regions of the Ramachandran plot and the overall geometry was better than average when compared to structures solved at the same resolution. Model refinement statistics are given in Table 1. The atomic coordinates and structure factors for the POZ^{LRF} structure have been deposited in the Protein Data Bank (PDB) [26] with Accession Code 2IF5.

Results and discussion

Overall, the structures of POZ^{LRF}, POZ^{PLZF}, and POZ^{BCL6} are very similar with root mean square deviation values of ≈1 Å between their backbone atoms (Fig. 1B). The core of the domain is formed by five α-helices, which are flanked by two small β-sheets. No discernable electron density was observed for loop residues 65–69 of POZ^{LRF}. There are three peaks in the crystal structure where the electron density exceeds 10 sigmas, indicating the presence of several heavy atoms. Praseodymium(III) ions were assigned to these peaks.

The biological unit of all three POZ domains appears to consist of a compact homodimer with an extensive interface that involves intermolecular β-strand interactions along with contributions from several α-helices. The dimers are distinctly non-globular, with dimensions of $55 \times 32 \times 29$ Å^3 for POZ^{LRF} (Fig. 1C). The dimer interface buries ∼1600 Å^2 of surface area per monomer in POZ^{LRF}, whereas the corresponding values are ∼1700 Å^2 and ∼2000 Å^2, respectively, in the POZ^{BCL6}, and POZ^{PLZF} homodimers. The most striking feature of the dimer interface is the domain-swapped strand β1 that forms an antiparallel β-sheet with strand β5 from the other molecule. The domain-swapping is almost certainly not an artifact of crystallization because it occurs in all three POZ domain structures determined to date. In fact, the structure of POZ^{BCL6} in complex with a SMRT-binding peptide revealed that the swapped β-strands constitute an integral part of the two pockets required for co-repressor binding [16].

Located between the two monomers of POZ^{LRF} is a pocket that contains the conserved residues Asp34, His47, and Arg48 (Fig. 1A). In POZ^{BCL6}, this pocket was originally thought to be involved in the recruitment of co-repressor SMRT [27]. Accordingly, even very conservative mutations inside the pocket, such as the substitution of a lysine for an arginine, clearly interfered with the interaction between POZ^{BCL6} and SMRT. However, when the crystal structure of POZ^{BCL6} in complex with a SMRT-derived peptide epitope was later determined, the peptide was found to form a 2:2 complex with POZ^{BCL6}, and the peptides were bound within two shallow lateral grooves that are located on the opposite face of the POZ domain with respect to the charged pocket [28]. These symmetry-related grooves are also composed of residues from both monomers, most notably domain-swapped strand β1. Remarkably, while the residues in the aforementioned charged pocket are conserved among the POZ domains of LRF, PLZF, and BCL6, there is significant sequence divergence between amino acids that line the lateral grooves. Overall, the general physiochemical characteristics of only 12 of 23 residues in the lateral grooves are conserved in the POZ domains of LRF and PLZF. PLZF is also known to associate with SMRT, but this requires the full-length PLZF protein and does not seem to involve the same epitope of SMRT [27]. Furthermore, in the same study BCL6 exhibited greater than 10-fold higher affinity for SMRT than PLZF. The sequence differences within the lateral grooves between LRF and BCL6 are even more striking than those between BCL6 and PLZF, with reversed charges in two

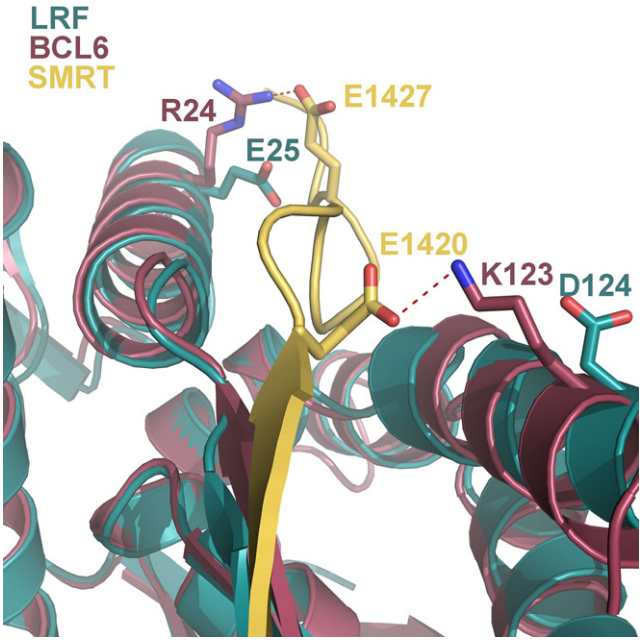

Fig. 2. BTB^{BCL6}-SMRT-binding interactions. Hydrogen-bonding interactions between two residues of POZ^{BCL6} and the SMRT-derived peptide are highlighted and the corresponding residues in POZ^{LRF} are superimposed to demonstrate that POZ^{LRF} is unlikely to bind SMRT in a similar fashion.

positions. Residues E25 and D124 in LRF superimpose well with R24 and K123 in POZ^{BCL6}, respectively, the latter pair of which form short side-chain-mediated hydrogen bonds with negatively charged E1427 (2.5 Å apart) and E1420 (3.2 Å apart) of the SMRT peptide (Fig. 2). Therefore, if LRF recruits SMRT at all, it almost certainly does so via a different mode of interaction. Of course LRF may utilize its lateral grooves for specific binding and recruitment of co-repressor molecules other than SMRT.

One of the more intriguing properties of POK-family proteins is their ability to form hetero- as well as homo-oligomers. For example, PLZF and BCL6 have been shown to interact *in vivo* [29] and an interaction between LRF and BCL6 was demonstrated by yeast two-hybrid experiments [1]. In the latter study, it was also observed that LRF did not interact with PLZF. The POZ domains by themselves were sufficient to mediate homodimerization of each protein, but the formation of LRF/BCL6 hetero-oligomers required the full-length proteins. This suggests that one or more regions outside of the POZ domains are necessary for the formation of hetero-oligomers. However, an LRF deletion mutant lacking only its POZ domain was unable to form hetero-oligomers with full-length BCL6 [1]. Thus, hetero-oligomerization of POK family proteins evidently involves both their POZ domains and at least one other region of the molecules.

The ability of LRF and PLZF to interact with BCL6 but not with each other may be due to the differing electrostatic properties of their POZ domains. Whereas both POZ^{LRF} and POZ^{PLZF} have an abundance of negatively charged surface residues (Fig. 3), which is also reflected in their theoretical isoelectric points (p*I*) of 4.4 and 4.9, respectively, the surface of POZ^{BCL6} displays a more balanced distribution of positive and negative charges (p$I = 7.0$). Hence, a potentially greater degree of electrostatic repulsion between

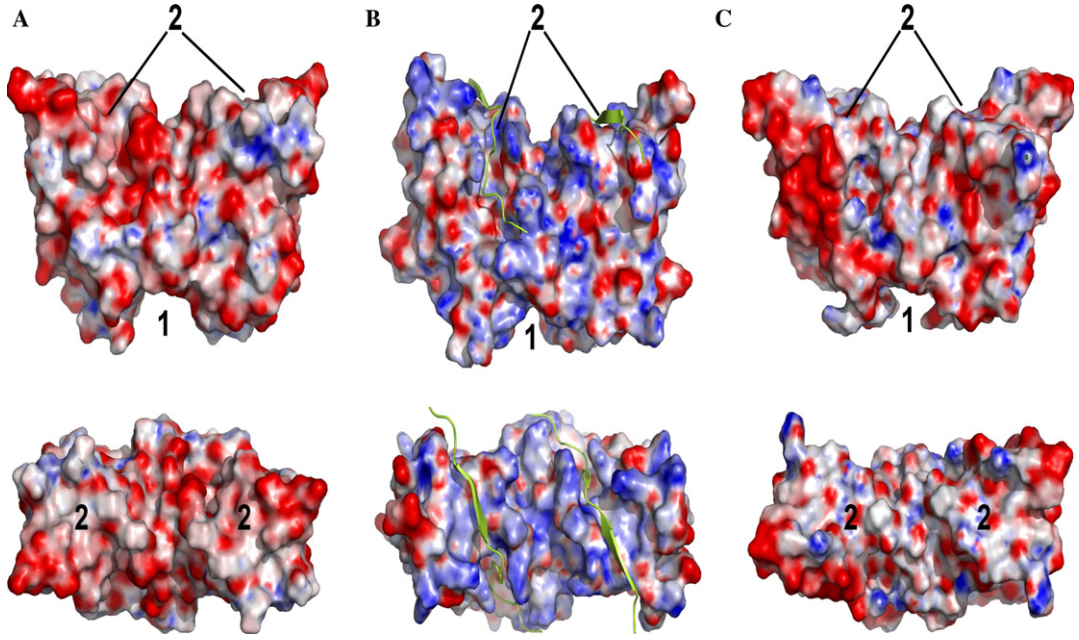

Fig. 3. Electrostatic surface representations of (A) POZ^{LRF}, (B) POZ^{BCL6}, and (C) POZ^{PZLF}. The conserved pocket at the dimer interface and shallow lateral grooves in each structure are labeled 1 and 2, respectively. In the case of POZ^{BCL6}, the SMRT peptide is also displayed to aid in the visualization of the shallow-binding grooves. The dramatic difference between the distribution of charged residues on the surface of POZ^{BCL6} compared to those of POZ^{LRF} and POZ^{PZLF} may play a role in dictating the specificity of hetero-oligomerization.

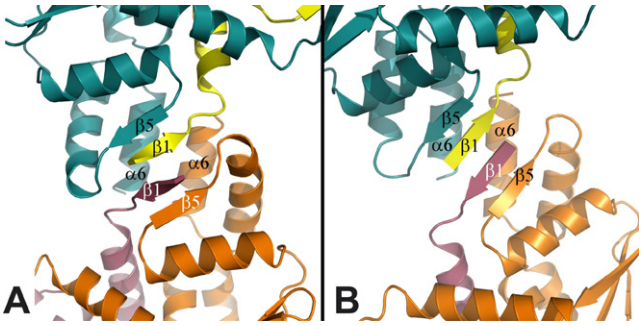

Fig. 4. Comparison of packing interactions in crystals of (A) POZ^{LRF} and (B) POZ^{BCL6}. In both cases, contacts between adjacent dimers are mediated primarily by strand–strand interactions involving strands from all four monomers. Further similarities between the packing arrangements observed in the POZ^{LRF} and POZ^{BCL6} crystals, including interactions between the two α6 helices, suggest that the same structural elements might facilitate LRF/BCL6 complex formation. (This figure and all previous figures with the exception of Fig. 1C were generated with PYMOL [33]).

LRF and PLZF than between either of them and BCL6 may dictate the specificity of the interactions.

A clue as to which parts of their respective POZ domains may participate in the interaction between LRF and BCL6 might be drawn from remarkable similarities in the packing arrangements between the POZ^{LRF} and POZ^{BCL6} crystals. Previously, Li et al. [17,18] and Ahmad et al. [17] observed conserved packing interactions in different crystal forms of the POZ^{PLZF} structure. These interactions involve the formation of a four-stranded β-sheet, with four adjacent molecules contributing one strand each. A similar packing arrangement was later observed in one crystal form of POZ^{BCL6} [16]. In both cases the authors discussed the possibility that these contacts might contribute to the oligomerization of the individual proteins. Because similar intermolecular interactions are also present in the POZ^{LRF} structure, we considered their potential role in the formation of hetero-oligomers between LRF and BCL6. The similarities between the packing arrangements of POZ^{BCL6} and POZ^{LRF} are intriguing in this regard. In both cases, the interface between dimers involves interactions between two β1 strands from molecules A and C, and the two α6 helices from molecules B and D (Fig. 4). The same structural components could conceivably be involved in BCL6/LRF complex formation. The BCL6/LRF interface would require a small structural rearrangement, however, because simple superposition of a POZ^{BCL6} dimer onto a second POZ^{LRF} dimer produces a steric clash between the C-terminus of POZ^{BCL6} and helix α1 of POZ^{LRF}.

Because the opposite sides of each symmetric dimer engage in the same contacts with still other dimers, these interactions could mediate the formation of higher-order oligomers. This could explain the observation that LRF and BCL6 seem to assemble into large, poorly defined oligomeric complexes *in vivo* [1]. However, as Ahmad et al. pointed out [16], the intermolecular strand–strand interactions between the dimers block a significant portion of the observed SMRT-binding site, and so the respective interactions of LRF and SMRT with BCL6 would be mutually exclusive.

In view of its essential role in oncogenic transformation [8], LRF may be an attractive molecular target for human cancer therapy. Interfering with the oligomerization of its POZ domain, or with the ability of POZ^{LRF} to recruit co-repressors, are two possible means of inhibiting the activity of LRF in cancer cells. Indeed, Polo et al. [30] have developed a peptide that binds to the lateral grooves of POZ^{BCL6} and abrogates co-repressor binding, thereby blocking its function. A similar strategy may also lead to the development of LRF inhibitors. The availability of the crystal structure of POZ^{LRF} can be expected to facilitate the identification of small molecule inhibitors by in silico screening or rational design.

Acknowledgments

We thank Kerri Penrose and Scott Cherry for technical support. This research was supported by the Intramural Research Program of the NIH, National Cancer Institute, Center for Cancer Research. Electrospray mass spectrometry experiments were conducted on the LC/ESMS instrument maintained by the Biophysics Resource in the Structural Biophysics Laboratory, NCI-Frederick. X-ray data were collected at the Southeast Regional Collaborative Access Team (SER-CAT) 22-ID beamline at the Advanced Photon Source, Argonne National Laboratory. Supporting institutions may be found at www.ser-cat.org/members.html. Use of the Advanced Photon Source was supported by the U.S. Department of Energy, Office of Science, Office of Basic Energy Sciences, under Contract No. W-31-109-Eng-38.

References

[1] J.M. Davies, N. Hawe, J. Kabarowski, Q.H. Huang, J. Zhu, N.J. Brand, D. Leprince, P. Dhordain, M. Cook, G. Morriss-Kay, A. Zelent, Novel BTB/POZ domain zinc-finger protein, LRF, is a potential target of the LAZ-3/BCL-6 oncogene, Oncogene 18 (1999) 365–375.

[2] R.T. Phan, R. Dalla-Favera, The BCL6 proto-oncogene suppresses p53 expression in germinal-centre B cells, Nature 432 (2004) 635–639.

[3] M. Barna, N. Hawe, L. Niswander, P.P. Pandolfi, Plzf regulates limb and axial skeletal patterning, Nat. Genet. 25 (2000) 166–172.

[4] L. Pasqualucci, O. Bereschenko, H. Niu, U. Klein, K. Basso, R. Guglielmino, G. Cattoretti, R. Dalla-Favera, Molecular pathogenesis of non-Hodgkin's lymphoma: the role of Bcl-6, Leuk. Lymphoma 44 (2003) S5–S12.

[5] C. Deweindt, O. Albagli, F. Bernardin, P. Dhordain, S. Quief, D. Lantoine, J.P. Kerckaert, D. Leprince, The LAZ3/BCL6 oncogene encodes a sequence-specific transcriptional inhibitor: a novel function for the BTB/POZ domain as an autonomous repressing domain, Cell Growth Differ.: Mol. Biol. J. Am. Assoc. Cancer Res. 6 (1995) 1495–1503.

[6] A.L. Shaffer, X. Yu, Y. He, J. Boldrick, E.P. Chan, L.M. Staudt, BCL-6 represses genes that function in lymphocyte differentiation, inflammation, and cell cycle control, Immunity 13 (2000) 199–212.

[7] A. Zelent, Translocation of the RAR alpha locus to the PML or PLZF gene in acute promyelocytic leukaemia, Br. J. Haematol. 86 (1994) 451–460.
[8] T. Maeda, R.M. Hobbs, P.P. Pandolfi, The transcription factor Pokemon: a new key player in cancer pathogenesis, Cancer Res. 65 (2005) 8575–8578.
[9] T. Maeda, R.M. Hobbs, T. Merghoub, I. Guernah, A. Zelent, C. Cordon-Cardo, J. Teruya-Feldstein, P.P. Pandolfi, Role of the proto-oncogene Pokemon in cellular transformation and ARF repression, Nature 433 (2005) 278–285.
[10] V.J. Bardwell, R. Treisman, The POZ domain: a conserved protein-protein interaction motif, Genes Dev. 8 (1994) 1664–1677.
[11] C.W. Wong, M.L. Privalsky, Components of the SMRT corepressor complex exhibit distinctive interactions with the POZ domain oncoproteins PLZF, PLZF-RARalpha, and BCL-6, J. Biol. Chem. 273 (1998) 27695–27702.
[12] P. Dhordain, R.J. Lin, S. Quief, D. Lantoine, J.P. Kerckaert, R.M. Evans, O. Albagli, The LAZ3(BCL-6) oncoprotein recruits a SMRT/mSIN3A/histone deacetylase containing complex to mediate transcriptional repression, Nucleic Acids Res. 26 (1998) 4645–4651.
[13] K.D. Huynh, W. Fischle, E. Verdin, V.J. Bardwell, BCoR, a novel corepressor involved in BCL-6 repression, Genes Dev. 14 (2000) 1810–1823.
[14] G. David, L. Alland, S.H. Hong, C.W. Wong, R.A. DePinho, A. Dejean, Histone deacetylase associated with mSin3A mediates repression by the acute promyelocytic leukemia-associated PLZF protein, Oncogene 16 (1998) 2549–2556.
[15] C. Lemercier, M.P. Brocard, F. Puvion-Dutilleul, H.Y. Kao, O. Albagli, S. Khochbin, Class II histone deacetylases are directly recruited by BCL6 transcriptional repressor, J. Biol. Chem. 277 (2002) 22045–22052.
[16] K.F. Ahmad, A. Melnick, S. Lax, D. Bouchard, J. Liu, C.L. Kiang, S. Mayer, S. Takahashi, J.D. Licht, G.G. Privâe, Mechanism of SMRT corepressor recruitment by the BCL6 BTB domain, Mol. Cell 12 (2003) 1551–1564.
[17] K.F. Ahmad, C.K. Engel, G.G. Privâe, Crystal structure of the BTB domain from PLZF, Proc. Natl. Acad. Sci. USA 95 (1998) 12123–12128.
[18] X. Li, H. Peng, D.C. Schultz, J.M. Lopez-Guisa, F.J. Rauscher 3rd, R. Marmorstein, Structure-function studies of the BTB/POZ transcriptional repression domain from the promyelocytic leukemia zinc finger oncoprotein, Cancer Res. 59 (1999) 5275–5282.
[19] Z.M. Otwinowski, W., HKL2000, Methods Enzymol. 276 (1997) 307–326.
[20] A.J. McCoy, R.W. Grosse-Kunstleve, L.C. Storoni, R.J. Read, Likelihood-enhanced fast translation functions, Acta Crystallogr. D, Biol. Crystallogr. 61 (2005) 458–464.
[21] T.A. Jones, J.-Y. Zou, S.W. Cowan, M. Kjeldgaard, Improved methods for building protein models in electron density maps and the location of errors in these models, Acta Crystallogr. A 47 (1991) 110–119.
[22] G.N. Murshudov, A.A. Vagin, E.J. Dodson, Refinement of macromolecular structures by the maximum-likelihood method, Acta Crystallogr. D 53 (1997) 240–255.
[23] S.D. Laboratory, Collaborative Computational Project, No. 4. 1994, The CCP4 suite: programs for protein crystallography, Acta Crystallogr. D 50 (1994) 760–763.
[24] A. Perrakis, R. Morris, V.S. Lamzin, Automated protein model building combined with iterative structure refinement, Nat. Struct. Biol. 6 (1999) 458–463.
[25] R.A. Laskowski, M.W. MacArthur, D.S. Moss, J.M. Thornton, PROCHECK: a program to check the stereochemical quality of protein structures, J. Appl. Crystallogr. 26 (1993) 283–291.
[26] H.M. Berman, J. Westbrook, Z. Feng, G. Gilliland, T.N. Bhat, H. Weissig, I.N. Shindyalov, P.E. Bourne, The Protein Data Bank, Nucleic Acids Res. 28 (2000) 235–242.
[27] A. Melnick, G. Carlile, K.F. Ahmad, C.L. Kiang, C. Corcoran, V. Bardwell, G.G. Prive, J.D. Licht, Critical residues within the BTB domain of PLZF and Bcl-6 modulate interaction with corepressors, Mol. Cell. Biol. 22 (2002) 1804–1818.
[28] T.C. Terwilliger, J. Berendzen, Automated MAD and MIR structure solution, Acta Crystallogr. D 55 (Pt 4) (1999) 849–861.
[29] P. Dhordain, O. Albagli, N. Honore, F. Guidez, D. Lantoine, M. Schmid, H.D.A. Zelent, M.H. Koken, Colocalization and heteromerization between the two human oncogene POZ/zinc finger proteins, LAZ3 (BCL6) and PLZF, Oncogene 19 (2000) 6240–6250.
[30] J.M. Polo, T. Dell'Oso, S.M. Ranuncolo, L. Cerchietti, D. Beck, G.F. Da Silva, G.G. Prive, J.D. Licht, A. Melnick, Specific peptide interference reveals BCL6 transcriptional and oncogenic mechanisms in B-cell lymphoma cells, Nat. Med. 10 (2004) 1329–1335.
[31] A.T. Brunger, Free *R* value: a novel statistical quantity for assessing the accuracy of crystal structures, Nature 355 (1992) 472–475.
[32] P. Gouet, E. Courcelle, D.I. Stuart, F. Metoz, ESPript: analysis of multiple sequence alignments in PostScript, Bioinformatics 15 (1999) 305–308.
[33] W.L. DeLano, The PyMOL Molecular Graphics System., DeLano Scientific LLC, San Carlos, CA, USA, 2001. http://www.pymol.org.